Earthquake Engineering, Tenth World Conference © 1992 Balkema, Rotterdam. ISBN 90 5410 060 5

Effect of strain rates on strength and mode of failure of R/C members

Hiroshi Hosoya, Isamu Abe, Kenji Yasui & Yuji Funayama
Tsukuba Research Institute, Okumura Corporation, Japan

ABSTRACT: In order to investigate the effect of strain rates on strength and mode of failure of reinforced concrete, column specimens were tested during either static or dynamic loading. Modes of failure of all M type specimens designed for flexural failure were similar for both static and dynamic loading, but the procedures of failure were influenced by strain rates on S type specimens designed for shear failure. The Q-δ curves were similar for M type, the curve during static loading was different from the ones during dynamic loading for S type. Maximum strengths during dynamic loading were 1.1~1.2 times greater than during static loading. When material strengths increased with the increase of the strain rates during dynamic loading, the calculated maximum strength values for M type were similar to the experimental values, but those for S type were about 25 % smaller than the experimental values.

1 INTRODUCTION

The material strengths of concrete and steel increase with the increase of the strain rates during dynamic loading(Iwai,1982). The relationship of load and displacement, the strength and the mode of failure of reinforced concrete members are influenced by loading rates during the dynamic loading (Kitagawa,1984 and Fujii,1986). This influence was examined from the standpoint of strain rates. However, at present there is no sufficient data available to fully document this effect. The main objective of this study was to investigate this effect of strain rate on strength and mode of failure by testing 12 prepared column specimens under either static or dynamic loading.

2 OUTLINE OF TEST

2.1 Specimens

Table 1 lists the specimen dimensions, and characteristics, along with the loading test conditions for each specimen. Schematic diagrams of the column specimens used in this study are shown in Fig. 1. The tests in this study were composed of two series labeled series ① and ②, with each series composed the M type specimens(No.1,2,3,7,8,9), designed for flexural failure, and the S type specimens(No.4,5,6,10,11,12), designed for shear failure. Each type was composed of three specimens, with one used for the static loading test, and the other two used for the dynamic loading tests. The total number of specimens was 12: 3 samples x 2 series(① and ②) x 2types(M and S). The cross section of column was 25 cm x 25 cm with a height of column 100 cm for the M type specimens, and 65 cm for the S type specimens. The total longitudinal reinforcement ratio was 2.44 % for either specimen type. The shear reinforcement ratio was 1.28 % for the M type specimen, 0.51 % for the S type specimen.

Table 1. Test specimen, characteristics and test loading conditions

Series		Series①		Series②	
Specimen type		M Type	S Type	M Type	S Type
bxD	(cm)	25x25	25x25	25x25	25x25
h=2a	(cm)	100	65	100	65
Longitudinal reinforcement		12-D13	12-D13	12-D13	12-D13
Pg	(%)	2.44	2.44	2.44	2.44
Pt	(%)	0.813	0.813	0.813	0.813
Shear reinforcement	(mm)	4-D6 @40	2-D6 @50	4-D6 @40	2-D6 @50
Pw	(%)	1.28	0.51	1.28	0.51
Shear span ratio	(a/D)	2.00	1.30	2.00	1.30
ACL	Static Loading	$0.3bD\sigma_B$		Following average axial load history during dynamic loading tests	
	Dynamic Loading	Initial load: $0.3bD\sigma_B$ During lateral loading: self-operated control by a hydraulic jack			
ASDR (cm/s)	Static Loading	0.01 [No.1]	0.01 [No.4]	0.01 [No.7]	0.01 [No.10]
	Dynamic Loading	10.0 [No.2] [No.3]	10.0 [No.5] [No.6]	10.0 [No.8] [No.9]	10.0 [No.11] [No.12]

b: Width of column; D: Depth of column; h: Height of column; σ_B: Compressive strength of concrete; Pg: Total longitudinal reinforcement ratio; Pw: Shear reinforcement ratio; Pt: Longitudinal reinforcement ratio; ACL: Axial compressive load; [ ]: Specimen number; ASDR: Average story displacement rate (cm/sec).

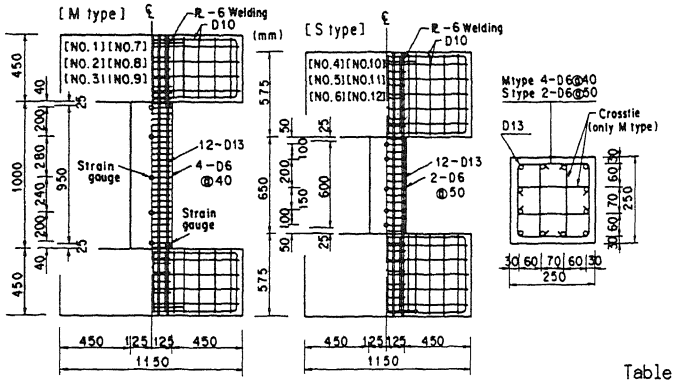

Figure 1. Column specimens details

2.2 Material properties

The material properties of the concrete are shown in Table 2, and those of the reinforcing bars are shown in Table 3. Compressive strengths of the concrete for the column specimens were 27.9 MPa ~30.9 MPa. Deformed bars of SD295 were used as the longitudinal and shear reinforcements. Yield strengths were 322 MPa for the longitudinal reinforcing bars and 359 MPa for the shear reinforcing bars. These properties were obtained using the test method of the Japanese Industrial Standard (JIS).

2.3 Test loading apparatus and test loading method

The loading apparatus is shown in Fig. 2. The loading conditions are shown in Table 1. Horizontal cyclic loading was applied by a computer controlled servo-actuator that followed the story displacement angle history as shown in Fig. 3. The story displacement angles were provided by sine waves with gradually increasing amplitude levels. The target value of the average story displacement rate $\tilde{V}$ of each cycle was 0.01 cm/sec during the static loading for specimens No.1, 4,7,10, and 10 cm/sec during the dynamic loading for specimens No.2,3,5,6,8,9,11,12. The latter was derived from the results of dynamic analyses of a reinforced concrete structure. The axial load for each column was applied by a hydraulic jack. For the series ①, axial loads were kept as constant as possible. Initial axial compressive load levels were 0.3 $bD\sigma_B$, where bD is the cross sectional area of column, and σ_B is the compressive strength of concrete. However, in reality the axial loads fluctuated during the dynamic loading tests. For series ②, in order to adjust the axial load level of each specimen, the axial load history for the static loading test followed the average axial load histories for the dynamic loading tests for each type group.

Table 2. Material properties of concrete

Series	Type	Specimen	Compres. strength (MPa)	Tensile strength (MPa)	Secant modulus (MN/cm^2)
①	M	No. 1	30.9	2.59	2.20
		No. 2	30.9	3.11	2.16
		No. 3	30.4	2.81	2.15
	S	No. 4	28.9	2.67	2.01
		No. 5	30.2	2.64	2.09
		No. 6	29.3	2.62	1.98
②	M	No. 7	28.3	2.57	1.94
		No. 8	27.9	2.58	1.90
		No. 9	28.7	2.41	1.91
	S	No. 10	30.4	2.43	1.99
		No. 11	29.5	2.46	1.93
		No. 12	29.8	2.42	1.86

Test method: JIS A 1108; Compres.: Compressive

Table 3. Material properties of reinforcing bars

Bar size	Yield strength (MPa)	Yield strain ($\times 10^{-6}$)	Ultimate strength (MPa)	Elastic modulus (MN/cm^2)	Elongation (%)
D13[1]	322	1840	478	17.85	28.1
D6[2]	359	2490	538	17.65	22.4

Test method: JIS Z 2241; 1) Longitudinal reinforcement 2) Shear reinforcement

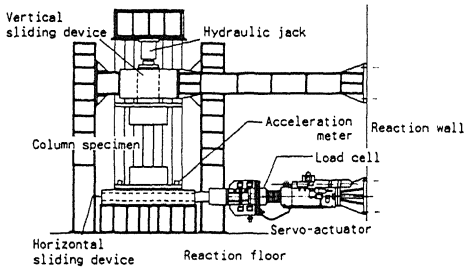

Figure 2. Loading apparatus

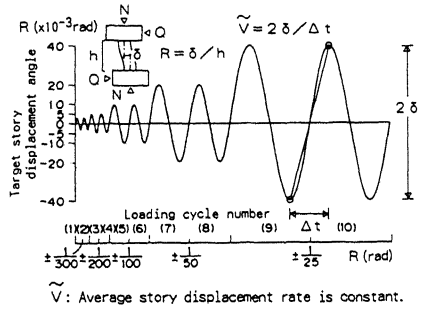

$\tilde{V}$: Average story displacement rate is constant.

Figure 3. Story displacement angle history

2.4 Instrumentation

Horizontal load values were measured with a load cell that was mounted on the servo-actuator. These values were corrected by using force of inertia values obtained with acceleration meters. Axial load values were measured with a pressure gauge of the hydraulic jack. Displacement of the column was measured with inductive displacement transducers installed in the middle of each column. Strain gauges were attached to both longitudinal reinforcing bars and shear reinforcing bars.

3 RESULTS AND DISCUSSION

3.1 Strain rates

The relationships of load and strain rate (Q-$\dot{\varepsilon}$ curves) and corresponding time histories of specimens No.8 and 12 are shown in Fig. 4. The strains were obtained by the strain gauges attached to the longitudinal reinforcing bars, and the strain rates were defined by the changing values of strain per unit time. During the dynamic loading, the maximum strain rates of both the M type and the S type specimens were $3\sim6\times10^4$ μ/sec. These strain rates corresponded to those that a structure would experience during an earthquake. Though the strain rates decreased at the load peak, they were about $2\sim3\times10^4$ μ/sec just prior to the peak.

3.2 Modes of failure

Final crack patterns of the M type specimens No.7 and 8, and the S type specimens No.4,10, 11 and 12 are shown in Fig. 5. The modes of failure of each type are explained below.
M type: Though the number of cracks during the static loading was greater than during the dynamic loading, crushing of concrete and mode of failure were similar for both the static and the dynamic loading. All M type specimens experienced flexural failure.
S type: Many shear cracks appeared and width of the cracks gradually increased; the longitudinal reinforcements buckled and shear reinforcements sprawled during the static loading. Several wide shear cracks appeared before a number of narrow shear cracks, the buckle and sprawl of reinforcements did not occur during the dynamic loading. During the static loading, specimen No.10 could not support the axial load on the 9th horizontal loading cycle at story displacement angle R= 1/25 radian, so the horizontal loading to the specimen was discontinued. Specimens No. 4,6,10 and 11 experienced shear failure and specimen No.5 experienced shear failure and flexural failure at the same time. Specimen No.12 experienced shear failure after the bond splitting cracks occurred along the longitudinal reinforcing bars. Though the mode of failure of all S type specimens was shear failure, the procedures of failure were influenced by strain rates.

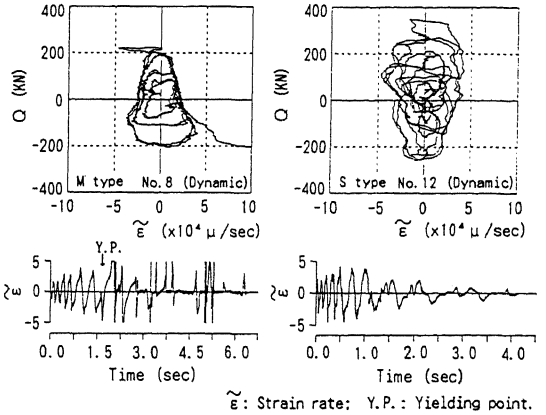

$\dot{\varepsilon}$: Strain rate; Y.P.: Yielding point.

Figure 4. Load - strain rate curves and time histories

3.3 Load - story displacement curves (Q-δ curves)

The Q-δ curves of the M type specimens No.7 and 8 and the S type specimens No.4,10,11 and 12 are shown in Fig. 6.
M type: The Q-δ curves during the static loading tests for the M type specimens were similar to the ones during the dynamic loading tests, except for the difference in maximum strengths. The Q-δ curves were only slightly influenced by the strain rates.
S type: The Q-δ curves of the S type specimen No.10 during the static loading test was different from the ones of other specimen of the same type. Because specimen No.10 was deformed much more than other specimens, it could not support the axial load during the loading test. The Q-δ curves of other S type specimens were similar during both the static and the dynamic loading tests, except for the difference in maximum strengths.
During the static loading, the shear rein-

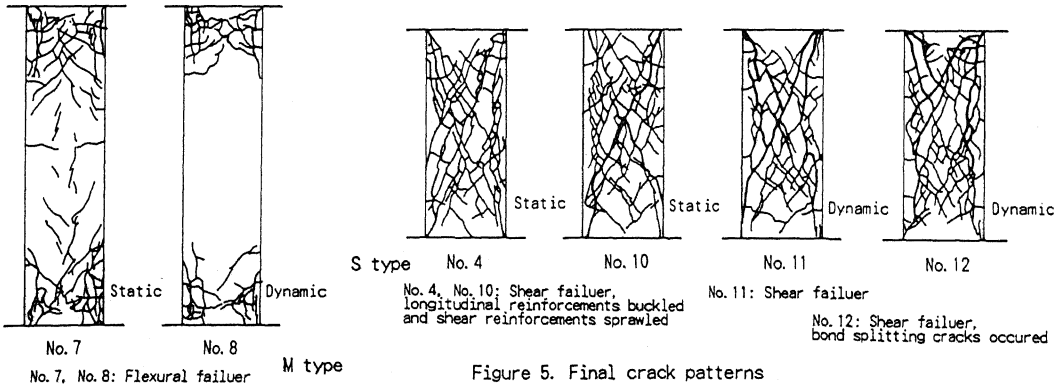

Figure 5. Final crack patterns

forcements yielded after the longitudinal reinforcements on specimens No.4 and 10. During the dynamic loading, the same behavior occurred on specimens No.5 and 6. During the dynamic loading for specimen No.11, the longitudinal reinforcements and shear reinforcements yielded at the same time. The longitudinal reinforcements yielded after the shear reinforcements for specimen No.12. Therefore, for the S type specimens, the yield behavior of reinforcements changed during the dynamic loading.

3.4 Story displacement angles at yielding and at maximum strength

The story displacement angles at yielding of the longitudinal reinforcements, the members and story displacement angles at maximum strength for series ② are shown in Table 4. Because the axial load history during the static loading was similar to that during the dynamic loading on each specimen in this group, comparisons of the story displacement angles at yielding and at maximum strength, along with initial stiffness, maximum strengths, and energy ratios can be made.

Though the story displacement angles at yielding of the longitudinal reinforcement during the dynamic loading tests were 1.4 times greater than the one during the static loading test, the story displacement angles at yielding of members and at maximum strengths were 0.9 times smaller than the ones during the static loading test for the M type specimens. On the other hand, the story displacement angles of yielding of the longitudinal reinforcements and at maximum strengths duing the dynamic loading tests were 1.1～1.2 times greater than the ones during the static loading tests for the S type specimens. In the case of the dynamic loading for the M type specimens, the story displacements angles at yielding of the longitudinal reinforcements, the ones at yielding of members and at maximum strengths came close to each other. The story displacement angles at yielding of the longitudinal reinforcements during the dynamic loading increased 20 %～40 % more than the ones during the static loading, because the yield strains of the reinforcing bars increased with the increase of the strain rate.

3.5 Initial stiffness

Initial stiffness values are shown in Table 5. They were defined by the relationships of loads and story displacements at R=1/300 radian in the Q-δ curves(see Fig. 6). For the M type specimens, the average of the initial stiffness values during the dynamic loading tests was 1.11 times higher than that for the static loading test. For the S type specimens, the average of initial stiffness values during the dynamic loading

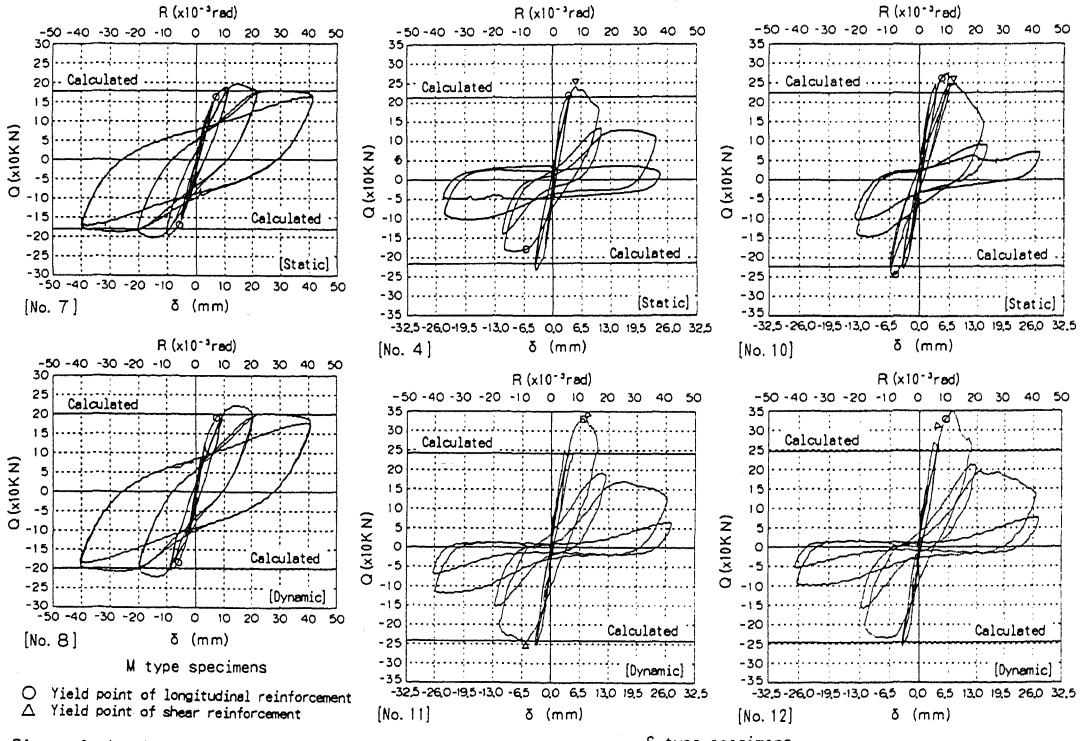

Figure 6. Load - story displacement curves (Q-δ curves)

Table 4. Story displacement angles

Type	Spec.	Load method	A R(rad)	Ratio*	B R(rad)	Ratio*	C R(rad)	Ratio*
M	No. 7	Stat.	1/196	1.0	1/103	1.0	1/70	1.0
	No. 8 No. 9	Dynam.	1/152 1/125	1.42	1/111 1/114	0.92	1/75 1/82	0.89
S	No. 10	Stat.	1/124	1.0	—	—	1/102	1.0
	No. 11 No. 12	Dynam.	1/ 89 1/114	1.22	— —	—	1/90 1/92	1.12

Spec.: Specimen; Stat.: Static loading; Dynam.: Dynamic loading;
A: Average of displacement angle at yielding of longitudinal reinforcement.
B: Average of displacement angle at yielding of a member.
C: Displacement angle at maximum strength of a member.

Table 5. Initial stiffness

Spec.	K_i (KN/mm)	Ratio*
No. 7	34.4	1.00
No. 8 No. 9	38.5 37.7	1.11
No. 10	86.0	1.00
No. 11 No. 12	93.7 95.8	1.10

Table 6. Maximum strengths

Spec.	Qtu (KN)	Ratio*
No. 7	201	1.00
No. 8 No. 9	218 220	1.09
No. 10	272	1.00
No. 11 No. 12	326 342	1.23

*: Ratio of displacement angle during dynamic loading to the one during static loading.
Ki: Initial stiffness; Qtu: Maximum strength;

tests was 1.10 times higher than that for the static loading test. Therefore, this increase was similar for both the M type and the S type specimens.

3.6 Maximum strengths

The maximum strengths of the series ② are shown in Table 6. For the M type specimens, the average of the maximum strengths during the dynamic loading tests was 1.09 times greater than that during the static loading test. For the S type specimens, the average of the maximum strengths during the dynamic loading tests was 1.23 times greater than that for the static loading test. Therefore, for both M and S type specimens, the maximum strengths increased during the dynamic loading under the influence of strain rates.

3.7 Energy ratios

The energy ratios of the series ② group are shown in Fig. 7. The energy ratio is defined as W/We, where W is the area of one cycle of hysteresis loop, and We is the equivalent potential energy. For the M type specimens, as the story displacement angle increased, the energy ratios also increased during both the static and dynamic loading. The energy ratios during the static loading were the same as those during the dynamic loading. For the S type specimens, as the story displacement angle increased to R=1/50 radian, the energy ratios also increased during both the static and dynamic loading. The energy ratios during the static loading were similar to those during the dynamic loading to R=1/100 radian. After R=1/50 radian, the decrease of energy ratio of the second cycle during the dynamic loading was much more than the one during the static loading.

3.8 Comparison between experimental and calculated values of maximum strength

The comparison between experimental and calculated values of maximum strength is shown in Table 7 and Fig. 8. The maximum flexural strengths and maximum shear strengths were

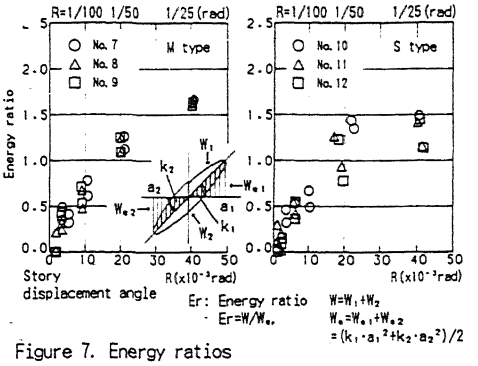

Figure 7. Energy ratios

calculated by the following equations(Architectural Institute of Japan, 1987).

Maximum flexural strength:

$$Qyu = 2/h\cdot[\Sigma a_{ti}\cdot {}_s\sigma_y\cdot g_1 + 0.5ND(1-N/bDF_c)] \quad \text{eq.(1)}$$

Maximum shear strength:

$$Qsu = [0.115\cdot k_u\cdot k_p(180+Fc)/(M/Qd+0.12) + 2.7\sqrt{(P_w\cdot {}_w\sigma_y)} + 0.1N/bd]bj \quad \text{eq.(2)}$$

where, Σa_{ti}: Tensile longitudinal reinforcement area; ${}_s\sigma_y$: Yield strength of longitudinal reinforcement; N: Axial load in column; b: Width of column; D: Overall depth of column; Fc: Compressive strength of concrete; h: Height of column; j: 7d/8; g_1: j/D; K_u=0.9; $k_p=0.82p_t^{0.23}$; p_t: Longitudinal reinforcement ratio; M/Qd: Shear span to effective depth ratio; d: Effective depth; P_w: Shear reinforcement ratio; ${}_w\sigma_y$: Yield strength of shear reinforcement.

The strengths of the concrete and reinforcing bars, obtained using the test method of JIS, were used to calculate the maximum strengths during the static loading. During the dynamic loading, the maximum strain rates were 2～3 x10^4 μ/sec just prior to the load peak. At these values, the compressive strengths of concrete during the dynamic loading material tests increased 1.2 times more than the ones during the static loading material tests. The yield strengths of the reinforcing bars during the dynamic loading material tests increased 1.15 times more than the ones during the static loading material tests(Iwai,1982). Therefore, when the maximum strengths during the dynamic loading tests were calculated, the strengths of concrete and reinforcing bars increased.

Table 7. Comparison between experimental and calculated values of maximum strengths

Series	Type	Spec.	Load	N (KN)	Experi. (KN) Qty (A)	Experi. (KN) Qtu (B)	Calculated (KN) Qyu (C)	Calculated (KN) Qsu (D)	Ratio (B/C)	Ratio (B/D)	MF
①	M	No. 1	Stat.	613	180	193	178	216	1.08	0.89	F
		No. 2	Dynam.	735	220	236	210	242	1.12	0.98	F
		No. 3	Dynam.	691	204	226	205	238	1.10	1.10	F
	S	No. 4	Stat.	530	—	237	257	213	0.92	1.11	S
		No. 5	Dynam.	686	319	324	314	248	1.03	1.31	FS
		No. 6	Dynam.	667	—	304	309	244	0.98	1.25	S
②	M	No. 7	Stat.	686	188	201	179	217	1.12	0.93	F
		No. 8	Dynam.	667	201	218	198	231	1.10	0.94	F
		No. 9	Dynam.	672	198	220	200	233	1.10	0.94	F
	S	No. 10	Stat.	618	—	272	274	224	0.99	1.21	S
		No. 11	Dynam.	657	—	326	308	243	1.06	1.34	S
		No. 12	Dynam.	691	—	342	314	247	1.09	1.38	S

Spec.: Specimen; Stat.: Static loading; Dynam.: Dynamic loading; Experi.: Experimental;
N: Axial load at maximum strength; Qty: Yield strength of member; Qtu: Maximum strength;
Qyu: Maximum flexural strength; Qsu: Maximum shear strength; MF: Mode of failure;
F: Flexural failure; S: Shear failure; FS: Shear failure after yield of member;
·The strengths of materials which were obtained with test method of JIS were used in calculation of static loading test values.
·The strengths of materials which increased with the increase of the strain rates were used in calculation of dynamic loading test values.

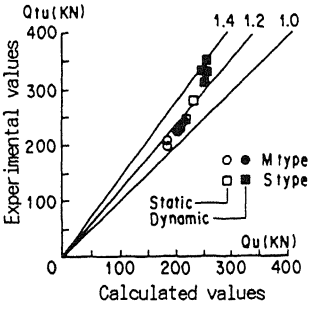

Figure 8. Comparsion between experimental and calculated values of maximum strengths

During the static loading test, the average of the experimental maximum strength values of the M type specimens No.1 and 7 (Qtu values in Table 7) was 1.10 times greater than the calculated maximum flexural strengths(Qyu). The average of the same values(Qtu) of the S type specimens No.4 and 10 was 1.16 times greater than the calculated maximum shear strengths(Qsu). For the dynamic loading tests, the average of the experimental maximum strengths of the M type specimens No.2,3,8,9 was 1.11 times greater than the Qyu value. The average of the experimental maximum strengths of the S type specimens No.5,6,11,12 was 1.32 times greater than the Qsu value.

When material strengths increased with the increase of the strain rates, the maximum strengths of the M type specimens calculated by using Eq.(1) were similar to the experimental values for both types of the loading tests. For the S type specimens, the maximum strengths calculated using Eq.(2) were about 25 % smaller than the experimental values obtained during the dynamic loading tests.

4 CONCLUSIONS

The column specimens were tested during either static or dynamic loading, and the effects of strain rates on strength and mode of failure were examined. The results can be summarized as follows:

(1) The maximum strain rates obtained during the dynamic loading were about $2\times10^{4}\,\mu$ /sec just prior to the load peak.

(2) For the flexural failure (M type) specimens, the mode of failure was similar for both static and dynamic loading. But for the shear failure (S type) specimens, the procedures of failure were different, since the mode of failure was influenced by strain rates.

(3) The Q-δ curves for the M type specimens were similar during the static and dynamic loading tests, but for the S type specimens, the curves differed during both the static and dynamic loading tests.

(4) Initial stiffness values for the dynamic loading tests were 1.1 times greater than that for the static loading test, for either the M type or the S type specimens.

(5) Maximum strengths during the dynamic loading tests were 1.09 times greater than the maximum strength during the static loading test for the M type and 1.23 times for the S type specimens.

(6) When material strengths increased with the increase of the strain rates, the calculated maximum strength values were similar to the experimental values obtained for the M type specimens, for the S type specimens, the calculated values were about 25 % smaller than the experimental values.

ACKNOWLEDGMENTS

The authors wish to express their appreciation to Prof. T.Okada and Mr. F.Kumazawa of University of Tokyo, and to Dr. Y.Kitagawa of Building Research Institute, Ministry of Construction for their guidance and advice.

REFERENCES

Architectural Institute of Japan. 1987. Data for ultimate strength design of reinforced concrete structures: 70-71. (in Japanese)

Fujii,S., et al. 1986. Effect of Loading rate on behavior of R.C. column(part I,II). Summaries of Technical Papers of Annual Meeting A.I.J.: 411-414. (in Japanese)

Iwai,T., et al. 1982. Effect of loading rate on the performance of structure elements - part I Effect of the strain rate on stress-strain relationships of concrete and steel-. Transactions of A.I.J. No.314: 102-111. (in Japanese)

Kitagawa,Y., et al. 1984. Dynamic response analyses with effects of strain rate and stress relaxation. Transactions of A.I.J. No.343: 32-41. (in Japanese)